Paleohydrological history of Lake Allos (2200 m a.s.l) since 13 500 cal a bp in the Mediterranean Alps inferred from an ostracod δ 18 O record

Rosine Cartier, Laurence Vidal, Florence Sylvestre, Corinne Sonzogni, Frédéric Guiter, Elodie Brisset, Cécile Miramont

DOI: 10.1002/jqs.3425

Paleohydrological history of Lake Allos (2200 m a.s.l) since 13 500 cal a BP in the Mediterranean Alps inferred from an ostracod $\delta^{18}O$ record

ROSINE CARTIER,[1,2]* LAURENCE VIDAL,[1] FLORENCE SYLVESTRE,[1] CORINNE SONZOGNI,[1] FRÉDÉRIC GUITER,[3] ELODIE BRISSET[3] and CÉCILE MIRAMONT[3]
[1]Aix-Marseille University, CNRS, IRD, Collège de France, INRAE. CEREGE, Europôle de l'Arbois, Aix-en-Provence, France
[2]Department of Geology, Lund University, Lund, Sweden
[3]Aix-Marseille University, CNRS, IRD, Avignon University. IMBE, Europôle de l'Arbois, Aix-en-Provence, France

Received 20 September 2021; Revised 8 March 2022; Accepted 11 March 2022

ABSTRACT: This paper presents the first Lateglacial/Holocene (the last 13 500 cal a BP) ostracod $\delta^{18}O$ record to infer hydroclimate variability in the Southern French Alps. *Cytherissa lacustris* ($\delta^{18}O_{sp}$) shells extracted from the sediments of Lake Allos allowed a reconstruction of $\delta^{18}O_{lake\ water}$ ($\delta^{18}O_{lw}$) except for the interval 5800–2800 cal a BP. The shape of the Younger Dryas (YD) clearly differed from records documented in the northern Alps. First, $\delta^{18}O_{lw}$ values remained close to modern values before a marked drop ca. 12 000 cal a BP. Then, after several oscillations, $\delta^{18}O_{lw}$ values increased, reaching the highest value of the record ca. 6100 cal a BP during a thermal optimum for this latitude. Finally, low $\delta^{18}O_{lw}$ values occurred from 450 to 100 cal a BP during the Little Ice Age (LIA) following the Medieval Climate anomaly. At the beginning of the YD, $\delta^{18}O_{lw}$ probably reflected changes in local glacier dynamics and precipitation sources. The following decrease in $\delta^{18}O_{lw}$ values was associated with higher freshwater inputs during the second half of the YD. During the LIA, the low $\delta^{18}O$ values are consistent with a higher torrential activity and lower air temperatures.

KEYWORDS: Lateglacial/Holocene; Mediterranean Alps; ostracods; oxygen isotopes; paleohydrology

Introduction

The Alpine climate has changed significantly during the past century, with temperatures increasing by 2 °C (Auer *et al.*, 2007), i.e. more than twice the global average. In the Southern French Alps, local climate conditions such as temperature, precipitation and wind are highly influenced by altitude, topography, and the relative contribution of air masses from the Atlantic Ocean and the Mediterranean Sea. For each of the most recent decades, the surface of the Mediterranean Sea has warmed by around 0.4 °C and sea level has risen by about 3 cm – comparable to global trends, but in part due to decadal variability related to the North Atlantic Oscillation (NAO) (Cramer *et al.*, 2018). The diversity of alpine environmental contexts requires a better understanding of local hydroclimate responses to climate change to improve regional climate prediction.

Climate variability exerts a strong control on regional alpine weather and local-scale environmental processes that are well recorded in past environmental studies (Blenckner *et al.*, 2007; Arnaud *et al.*, 2016; Cartier *et al.*, 2019; Regattieri *et al.*, 2019). Lake sediment deposits are excellent archives to study climate evolution because of the acute sensitivity of lakes to environmental change and multi-scale processes throughout the hydrological cycle (Schwander *et al.*, 2000). Therefore, producing oxygen isotope records from alpine lacustrine sediments allows a better understanding of high-altitude hydroclimate variability to compare with mid-European and Mediterranean records (von Grafenstein *et al.*, 1999; Zanchetta *et al.*, 2007; Magny *et al.*, 2007, 2011; Regattieri *et al.*, 2019). These regional comparisons can reveal local climate specificities through time as well as synchronicities and time lags in hydrological and environmental responses to global climate events (Lauterbach *et al.*, 2011).

In the Southern French Alps, long-term paleoclimate records remain scarce and/or do not cover the entire Lateglacial/Holocene periods (Harrison *et al.*, 1993; Digerfeldt *et al.*, 1997; Drysdale *et al.*, 2006; Wilhelm *et al.*, 2012; Wirth *et al.*, 2013; Cartier *et al.*, 2019; Regattieri *et al.*, 2019). Climate, environmental changes and vegetation succession that have occurred since the last glaciation are not entirely documented and understood (Brisset *et al.*, 2015; Cartier *et al.*, 2018). In the Mercantour Massif, deglaciation of cirque-glacier catchments occurred between 14 000 and 13 500 cal a BP, i.e. during the Lateglacial Interstadial (Brisset *et al.*, 2015). In the same area, several moraines suggest glacier advances during the Younger Dryas (YD) associated with wet conditions, a different signature from elsewhere in the Alpine region and indicative of a regional specificity (Pauly *et al.*, 2018; Spagnolo and Ribolini, 2019). The last retreat of a cirque glacier following deglaciation goes back to the beginning of the Holocene (ca. 11 000 cal a BP). Later, relatively wet conditions occurred during the Early and Late Holocene bracketed by drier conditions from ca. 7000 to 3000 cal a BP as suggested by lake level reconstructions and speleothem records (Harrison *et al.*, 1993; Digerfeldt *et al.*, 1997; Regattieri *et al.*, 2019). Even though the literature has indicated glacier advances during the Holocene (Subboreal and Little Ice Age, LIA; Federici *et al.*, 2017), no clear pattern is seen in lake sediment records (Brisset *et al.*, 2015). The watershed of Lake Allos (also in the Mercantour Massif) contains moraines which could be attributed to the Neoglacial period (ca. 4500 cal a BP) or the LIA (Jorda, 1975; de Beaulieu, 1977). In summary, questions remain regarding the local hydroclimate evolution in the Southern French Alps and its specificities at key periods of environmental changes.

*Correspondence: Rosine Cartier, 1Aix-Marseille University, as above.
Email: rosine.cartier@geol.lu.se

In this paper, we present the first $\delta^{18}O$ record covering the end of the Lateglacial, and Early and Late Holocene for the Mediterranean Alps, based on the analysis of ostracods buried in sediments from Lake Allos (2200 m a.s.l). The $\delta^{18}O$ signal in lake carbonates is a function of lake water oxygen isotope composition and temperature (Stuiver, 1970; Leng and Marshall, 2004). This relationship with lacustrine conditions has led to successful reconstructions of past $\delta^{18}O$ lake water ($\delta^{18}O_{lw}$) for Mediterranean lakes (Develle *et al.*, 2010; Roberts *et al.*, 2010). $\delta^{18}O_{lw}$ provides a regional paleoclimate proxy, not influenced by local human activities, allowing a comparison with environmental and geomorphological studies (glacier advances, Holzhauser *et al.*, 2005; Rea *et al.*, 2020; torrential activity, Brisset *et al.*, 2017; pollen assemblages, Cartier *et al.*, 2018) and large-scale climate oscillations in Europe (e.g. Younger Dryas, Medieval Climate Anomaly (MCA), LIA). Finally, the hydrological response of Lake Allos is compared to a large set of records from central Europe, the Northern/Southern Alps and the Mediterranean basin to highlight the specificities of the region.

Watershed and lake properties

Lake Allos (44°14′N, 6°42′35″E) is characterized by a 40-m-deep basin located in the subalpine zone at 2230 m a.s.l in the Mercantour national park 'Massif du Mercantour' in the Southern French Alps (Fig. 1). Lake Allos is the largest (1 km long and 700 m wide; 54 ha) natural mountain lake in Europe at an altitude above 2000 m. The lake is located in a karstic dissolution basin shaped by Quaternary glaciers (Cartier *et al.*, 2018). The watershed of 520 ha culminates at 2740 m a.s.l. It consists, upstream, of sandstones of Triassic to Cretaceous age building the highest parts, and carbonate conglomerates south of the lake. The watershed is covered by scratched grasslands associated with larches. Lake Allos is composed of two basins constrained by lithology. In the south, the deeper basin (46 m water depth) basement is composed of limestone and karstified calcareous marls; north, a carbonate conglomerate unit constrains a shallower basin (20 m water depth) (Fig. 2). The lower limit of these conglomerates corresponds to a Paleocene erosional surface and Late Cretaceous limestones. Precipitation and snowmelt in the drainage basin feed three major torrents (Laus, Lac and Source). There is no surface outlet and tidal range can reach 13 m on an annual cycle (ONEMA, 2013). A natural underground outlet in the northern part of the lake feeds the downstream torrent (Chadoulin), which stops flowing during dry summers when the lake level is below the outlet level. The surface of Lake Allos is generally frozen from November to May and lake waters are stratified during summer. Annual water temperature in the epilimnion varies between 8 and 15 °C. In the hypolimnion (below 15 m depth), water temperature varies between 3.6 and 4.3 °C (annual monitoring between June and September in 2013; ONEMA; Supporting Information Material S1).

Regional climate and oxygen isotope composition of precipitation

Climate in the Southern French Alps is temperate. Winter snow depths average 122 cm at 2700 m a.s.l. and snow cover duration is about 182 days at 2100 m a.s.l. (Durand *et al.*, 2009a). Mean annual temperature in the Southern French Alps at 1800 m a.s.l. is 4.8 °C, varying from −0.1 °C in winter to 9.6 °C in summer, and mean annual precipitation is 944 mm, mainly in spring and

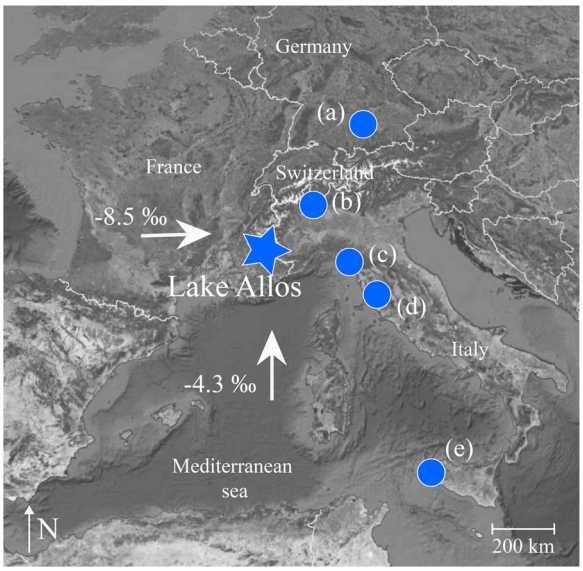

Figure 1. Location map of Lake Allos and other paleohydrological records discussed in the text: (a) Lake Ammersee (von Grafenstein *et al.*, 1999); (b) Lake Ghirla (Wirth and Sessions, 2016); (c) Corchia Cave (Zanchetta *et al.*, 2007); (d) Lake Accesa (Magny *et al.*, 2007); (e) Lake Preola (Magny *et al.*, 2011). The blue star shows the location of Lake Allos. White arrows indicate weighted mean $\delta^{18}O$ of rain from the Mediterranean region(-4.3 ‰) and the Atlantic (-8.5 ‰) (Celle-Jeanton *et al.*, 2004). [Color figure can be viewed at wileyonlinelibrary.com]

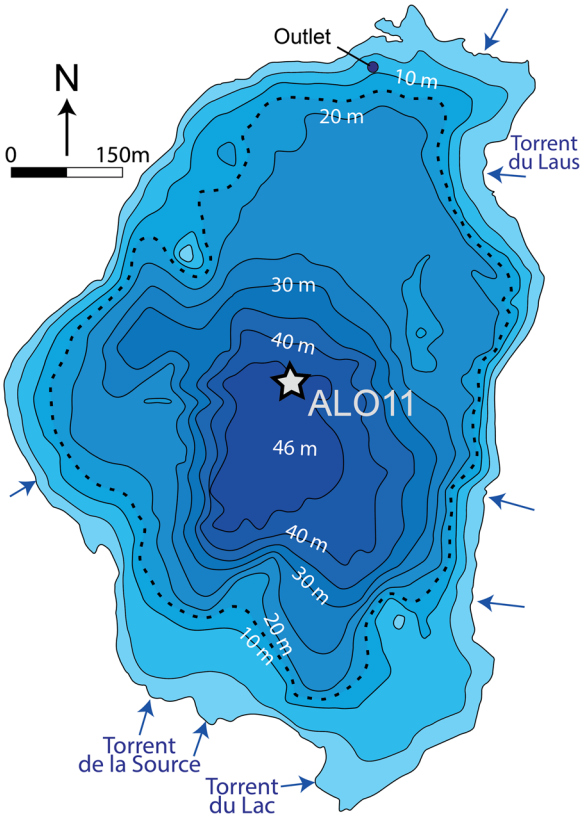

Figure 2. Bathymetry of Lake Allos (in meters) and location of the coring site (ALO11). Dark blue corresponds to deeper waters. The dashed line corresponds to a low lake level recorded in summer 2006. Arrows represent water inflows to the lake and the outlet is represented by a black dot. [Color figure can be viewed at wileyonlinelibrary.com]

autumn (Durand *et al.*, 2009b). The precipitation regime is characterized by a strong seasonality mainly determined by a north-westerly atmospheric flow and by the northward penetration of Mediterranean flows in the Southern Alps. The source

areas of alpine precipitation can be traced with oxygen isotopes because precipitation of Mediterranean origin has a mean weighted oxygen isotope composition of $\delta^{18}O_p = -4.3$ ‰ VSMOW (SD = 1.7 ‰), whereas those of Atlantic origin, which supply a large amount of rainfall during winter months (Bolle, 2003), have a $\delta^{18}O_p = -8.5$ ‰ VSMOW (SD = 3.51‰) (Fig. 1; Celle-Jeanton *et al.*, 2004).

Figure 3 shows monthly weighted means of $\delta^{18}O_p$ from GNIP stations around Lake Allos (IAEA/WMO, 2019 Thonon-les-Bains: 46°22′N, 6°28′E; Draix: 44°13′N, 6°33′E; Malaussène: 43°92′N, 7°13′E; Monaco: 43°73′N, 7°42′N). For Thonon-les-Bains (385 m a.s.l) and Draix (851 m a.s.l), two stations North-East of Lake Allos, mean $\delta^{18}O_p$ is −7.4 ‰ during summer months and −11.3 ‰ during winter months. South of Lake Allos and closer to the Mediterranean Sea, the mean $\delta^{18}O_p$ at Malaussène station (359 m a.s.l) is −5.8 ‰ during summer months and −4.9 ‰ during winter months; −2.18 ‰ and −5.85 ‰ for Monaco (2 m a.s.l), respectively (Fig. 3). At these stations, $\delta^{18}O_p$ values are not a function of the amount of precipitation but rather vary according to the season. $\delta^{18}O_p$ follows a linear relationship with air temperature (IAEA/WMO, 2019) and is lower during periods of lower air temperatures influenced by air masses from the Atlantic.

Methods

The long sediment sequence of Lake Allos was sampled in July 2011 (name: ALO11) in the deep (45 m), southern basin (44°14′N, 6°42′29″E) using a UWITEC piston-coring device mounted on a floating platform (laboratory EDYTEM). Four sites were cored (sites I to IV). The cored sediment sequences reached the geological basement at a coring depth of 14 m in sites 01 and 04, and at 13.5 m in site 03. In addition, a short core (ALO11-P1) was sampled using a UWITEC gravity corer to preserve the sediment interface. All the 18 core sections are presented in supplementary material in Cartier *et al.* (2018) and are available at https://doi.org/10.1016/j.quascirev.2018.02.016. Extensive figures are presented in Brisset *et al.* (2014) in open access at https://tel.archives-ouvertes.fr/tel-01095721. The chronology of core ALO11 is based on 23 accelerator mass spectrometry (AMS) ^{14}C dates (Cartier *et al.*, 2018) from terrestrial macro-remains measured by the Poznan Radiocarbon Laboratory and ^{210}Pb accumulation rate constrained by ^{137}Cs measured in the underground laboratory of Modane (Etienne *et al.*, 2013). Considering temporal deposition differences between continuous and instantaneous sediment layers, age–depth modeling was performed after removing flood layer thicknesses (see details in Cartier *et al.*, 2018).

Lake water sampling and measurements of δD and $\delta^{18}O_{lw}$

Lake water samples were collected directly after spring snowmelt and following the drier summer season to evaluate the effect of summer evaporation on $\delta^{18}O_{lw}$. Water sampling was performed at Lake Allos from the shore using 50-ml polyethylene dark bottles fully filled at the following dates: 23 September 2019, 9 June 2020 and 12 October 2020.

Measurements of δD and $\delta^{18}O_{lw}$ were performed in two laboratories because of logistic difficulties during the coronavirus pandemic. The sample collected in 2019 was measured at CEREGE (France) on a Picarro L2140i analyser coupled with a high-precision A0211 vaporizer and an A0325 autosampler. Standard deviation on routine measurements was ±0.023 ‰ for $\delta^{18}O$ and ±0.078 ‰ for δD. The two water samples taken in 2020 were measured at the BGS (British Geological Survey, UK). Oxygen isotope ($\delta^{18}O$) measurements were made using the CO_2 equilibration method with an Isoprime 100 mass spectrometer plus an Aquaprep device. Deuterium isotope (δD) measurements were made using an online Cr reduction method with a EuroPyrOH-3110 system coupled to a GVI IsoPrime mass spectrometer (Morrison *et al.*, 2001). Standard deviation was ±0.05 ‰ for $\delta^{18}O$ and ±1.0 ‰ for δD.

Extraction and preparation of ostracods for $\delta^{18}O$ analysis

Directly after coring (autumn 2011), the entire 14-m-long sequence (half cores of the sections 'OUT' correlated to the master core ALO11 at a maximum error range of 5 mm; see

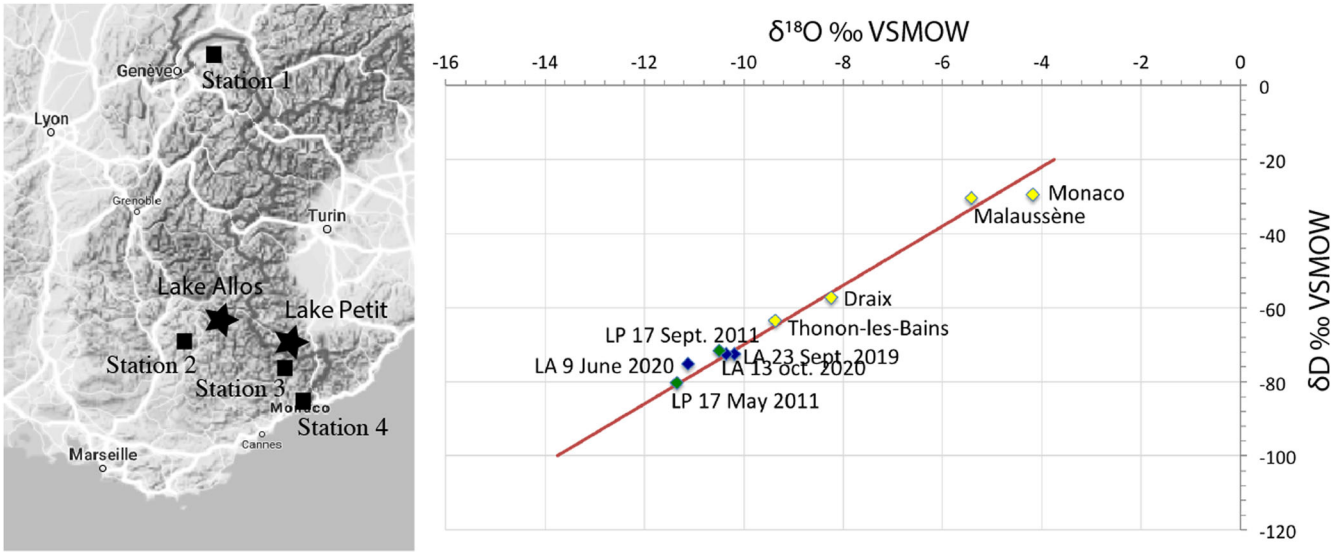

Figure 3. On the left, location map of meteorological stations (black squares) and lakes (stars). On the right, $\delta^{18}O$and δD (in ‰ VSMOW) in lake waters of Allos (in blue LA: 23 September 2019; 9 June 2020 and 13 October 2020) compared to other sites: Lake Petit (in green LP: 17 May 2011 and 17 September 2011; Cartier *et al.*, 2019); Mean $\delta^{18}O$ and δD in precipitation from meteorological stations (in yellow Station 1 Thonon-les-Bains 1999–2016, Station 2 Draix 2004–2013, Station 3 Malaussène 1997–1999 and Station 4 Monaco 1999–2016; IAEA/WMO, 2019). Thered line represents the global meteoric water line (GMWL). [Color figure can be viewed at wileyonlinelibrary.com]

supplementary material in Cartier *et al.*, 2018) was sliced continuously every 5 cm (270 samples in total). Each sample covers on average 30 years ([min;max] = [5;63], see the accumulation rate in Cartier *et al.*, 2018). The sample volume was 170 cm^3 above 564 cm and 77 cm^3 below. Samples were kept in closed bottles at low temperatures to maintain their humidity. All the 270 samples were analysed. Most samples were sieved from February to April 2012 and the remaining samples during autumn 2012. As the sediment was fresh and humid, hand-sieving with water was soft, allowing complete removal of detrital particles without mechanical or chemical actions. The sieved material was retrieved from 200- and 100-µm meshes with water, and ostracods were hand-picked with a fine brush using a stereo binocular microscope and Petri dishes. The ostracod valves were well preserved without any signs of mechanical stress or dissolution. Adhering sediments were removed using distilled water, fine needles and brushes. Then, carapaces were rinsed with ethanol and dried in ambient air (Caporaletti, 2011). All ostracods were counted and identified using a specific flora of Western and Central Europe (Meisch, 2000) to identify changes in ostracod abundances and ecology. These results have already been published in Cartier *et al.* (2018).

According to Cartier *et al.* (2018), *Cytherissa lacustris* valves are present in the sediments during periods of oligotrophic and oxic deep waters, whereas soil acidification and long-term cation release may have limited the calcification reaction from 5800 to 2800 cal a BP. *C. lacustris* is absent from the last centimetre of sediment and is replaced by the more eutrophic species *Cypria ophthalmica*.

Analysis of oxygen isotopes in C. lacustris ($\delta^{18}O_{sp}$) and reconstruction of $\delta^{18}O_{lw}$

Cleaned valves of *C. lacustris* were counted and weighed. The measurement of oxygen isotopes was performed on a minimum of three valves having a total mass >50 µg. Oxygen isotopes ($\delta^{18}O_{sp}$) were measured using a Kiel III Carbonate Device coupled to a Thermo Finnigan Delta Plus IRMS (in the CEREGE laboratory, Aix-en-Provence) and expressed in ‰ relative to VPDB. Based on NBS-19 measurements, the analytical precision for $\delta^{18}O$ is 0.06 ‰. For the reconstruction of $\delta^{18}O_{lw}$, $\delta^{18}O_{sp}$ values were corrected for various effects such as isotopic fractionation at equilibrium (expressed relative to SMOW; Coplen, 2007) and the vital effect. The vital effect of *C. lacustris* has been studied in two lakes, Starnberger See and Ammersee, at different stages of development and different depths (von Grafenstein *et al.*, 1999) and in Devriendt *et al.* (2017). Since the freshwater environment of Lake Allos is similar to that of Lake Ammersee, the vital effect calculated in von Grafenstein *et al.* (1999) was used in this paper. Based on this study, adults of *C. lacustris* are in average enriched by $+1.49 \pm 0.16$ ‰ VPDB relative to equilibrium calcite. The isotopic enrichment of waters by evaporation is considered negligible at Lake Allos (see Results and interpretation).

The oxygen isotope composition of lake waters ($\delta^{18}O_{lw}$) was then calculated as follows (Kim and O'Neil, 1997):

$$\delta^{18}Ow = \delta^{18}Osp - \Delta^{18}Ovo - \Delta^{18}O(C - H2O; 4°C) - \Delta^{18}Oe$$

where $\delta^{18}O_w$ is the oxygen isotope ratio in lake waters (‰ VSMOW), $\delta^{18}O_{sp}$ is the oxygen isotope ratio in ostracods and $\Delta^{18}O_{vo}$ is vital offset; ostracods enriched by $+1.49 \pm 0.16$ ‰ compared to an equilibrium calcite. After subtraction of the vital effect, $\delta^{18}O_{sp}$ values (‰ VPDB) were converted to the SMOW scale using the equation of Coplen *et al.* (1983):

$$\delta^{18}O \quad (VSMOW) = \quad 1,0309* \quad \delta^{18}O(VPDB) + 30.9$$

where $\Delta^{18}O_e$ is the enrichment by evaporation (considered negligeable at Lake Allos) and $\Delta^{18}O$ (C-H_2O; 4 °C) is the isotope fractionation equilibrium between calcite and water at 4 °C = 32.635 on the SMOW scale, calculated from the following equation with T = temperature in K (Kim and O'Neil, 1997):

$$\Delta^{18}O \quad (C - H2O; \quad 4°C) = 1000 \quad ln(\alpha) = 18.03 * \left(\frac{10^3}{T}\right) - 32.42$$

All reconstructed oxygen isotope values were corrected by −0.89 ‰ to account for the $\delta^{18}O$ difference between inorganic calcite precipitation according to Kim and O'Neil (1997) (used by von Grafenstein *et al.*, 1999 to calculate the vital effect of *C. lacustris*) and Friedman and O'Neil (1977) (Decrouy *et al.*, 2011).

Results and interpretation

Modern variability in $\delta^{18}O_{lw}$ and hydrological functioning of Lake Allos

A monitoring program of $\delta^{18}O_p$ carried out between 2004 and 2009 by the IAEA/WMO in 2015 was performed at Draix station (44°08′00″N, 006°20 ′00″E), located 25 km from Lake Allos (Supporting Information Material S1). Mean annual values of $\delta^{18}O_p$ varied between −7.0 ‰ (in 2006) and −10.4 ‰ (in 2009). Mean $\delta^{18}O_p$ for the 6 years of monitoring was −8.32 ‰.

The modern oxygen and deuterium isotope compositions of Allos' lake waters at different seasons of the year were compared to $\delta^{18}O$ and δD values in Lake Petit waters located nearby, and $\delta^{18}O_p$ values from weather stations in the region (Fig. 3). The values at Allos plot near the global meteoric water line and were slightly heavier than at Lake Petit during spring 2011 (Fig. 3).

In June 2020, $\delta^{18}O_{lw}$ (‰ VSMOW) at Allos was −11.1 ‰ (SD = 0.01 ‰) and δD (‰) was −75.1‰ (SD = 0.71 ‰). In September 2019, $\delta^{18}O_{lw}$ (‰ VSMOW) was −10.4 ‰ (SD = 0.06 ‰, two replicates) and δD (‰ VSMOW) was −72.6 ‰ (SD = 0.29 ‰, two replicates). The following year in October 2020, $\delta^{18}O_{lw}$ (‰ VSMOW) at Allos was −10.5 ‰ (SD = 0.01 ‰) and δD (‰ VSMOW) was −71.6 ‰ (SD = 0.43 ‰). Both samples in September and October plot on the global meteoric water line, showing no effect of lake water evaporation on the $\delta^{18}O$ and δD values of lake waters.

These results suggest that Lake Allos behaves like an open system with high dilution and fast discharge due to an underground outlet in the karstic depression. Considering an average Chadoulin flux of ~275 L s^{-1} (Carzon, 1958) and a volume of Lake Allos of ca. 9×10^6 m^3 based on the bathymetric data, the estimated water residence time is close to 1 year. Recent data (SAGE, 2014) provide a mean value of 112 L s^{-1} of the flux of Chadoulin over a 5-year survey. This gives a mean residence time of <2.5 years, similar to the estimation based on less recent data. In systems with a relatively short residence time of water, it is expected that $\delta^{18}O$ values of lake waters are primarily influenced by the $\delta^{18}O$

signature of direct precipitation (depending on air temperature at the time of precipitation formation and precipitation origin) and the $\delta^{18}O$ composition of the main water inflows from the watershed (i.e. snowmelt) (Roberts *et al.*, 2008). The lake level of Allos can temporarily drop below the underground outlet during dry summers, meaning that an effect of evaporation could play a role only during exceptional years. Annual lake water mixing occurs twice, once during spring snowmelt and once in late autumn, as in other deep lake systems such as Lake Ammersee in southern Germany (von Grafenstein *et al.*, 1996).

Significance of the C. lacustris $\delta^{18}O$ signal

Cytherissa lacustris (Cytherideidae) is an endobenthic species and inhabits sublittoral and profundal zones of cold, deep lakes and the littoral zones of high-altitude alpine lakes (Meisch, 2000). *C. lacustris* is very sensitive to oxygenation conditions prevailing at the sediment–water interface and maximum abundance is found in waters between 4 and 15 °C throughout the year. Adults and juveniles of *C. lacustris* are found together without seasonal changes in relative abundance, meaning that *C. lacustris* reproduces continuously throughout the year (von Grafenstein *et al.*, 1999). Therefore, variations in $\delta^{18}O_{sp}$ represent annual deep water variability.

According to annual monitoring (see Study site section and Supporting Information Material S1), deep lake waters of Lake Allos (below 15 m depth) where *C. lacustris* develops remained at 4 °C throughout 2013. Seismic surveys show that the lake sediment infill is well stratified with no evidence of sediment reworking (Wilhelm *et al.*, 2012). Layers of sediment are continuous between the shallow basin and the deep basin, suggesting that the lake level did not drop by more than 20 m over the study period. As lake water temperature is close to 4 °C below 15 m, we consider that temperature at the bottom of the deep basin remained relatively constant. Therefore, $\delta^{18}O_{sp}$ variations are assumed to be representative of $\delta^{18}O_{lw}$ variations. Note that samples cover a longer period (ca. 30 years) compared to the *C. lacustris* calcification timespan.

Reconstruction of past $\delta^{18}O_{lw}$

Thick and strongly calcified valves of *C. lacustris* are well preserved in the sediments and show no signs of dissolution (Fig. 4). *C. lacustris* is almost the only species of ostracods found in the sediments. Valves of *Cypridopsis vidua*, *Candona candida* and *Cypria ophthalmica* are present in sediments from the last 1500 years (Cartier *et al.*, 2018). Abundance of *C. lacustris* is variable along the core. Ostracod valves are absent in the sediments from 5800 to 2800 cal a BP during a period with high diatom concentrations (data published in Cartier *et al.*, 2018; Figure 5). Mean *C. lacustris* abundance in core sediment slices 5 cm long is 3.1 valves from the bottom to 5800 cal a BP and 2.8 valves from 2800 cal a BP to the top of the record (Cartier *et al.*, 2018). Concentrations in valves cm^{-3} are presented in Fig. 5. The highest concentrations, up to 0.35 valves cm^{-3}, are observed at the end of the YD and from 10 000 to 8500 cal a BP. *C. lacustris* valves were sufficiently numerous to allow 73 oxygen isotope measurements.

Over the entire study period, minimum and maximum values of $\delta^{18}O_{sp}$ range from −8.4 ‰ VPDB (11 900 cal a BP) to −6.3 ‰ VPDB (6100 cal a BP) (Fig. 5). Mean $\delta^{18}O_{sp}$ along the core is −7.1 ‰ VPDB (SD = 0.4‰). The highest variability in $\delta^{18}O_{sp}$ is observed during the YD (12 700–11 500 cal a BP). A drop in $\delta^{18}O_{sp}$ is present at 11 900 cal a BP and followed by an increase in $\delta^{18}O_{sp}$ at the transition with the Holocene. After a peak, values decrease again until ca. 8500 cal a BP. High $\delta^{18}O_{sp}$ values are present from 7200 to 6100 cal a BP, ca. 2800 cal a BP and ca. 1000 cal a BP during a thermal optimum for mid-northern latitudes and during the MCA. $\delta^{18}O_{sp}$ drops again to low values from 500 cal a BP during the LIA before a rise in the topmost sample representing sub-modern conditions (Fig. 5). Unfortunately, *C. lacustris* is absent from the first top centimetre of sediments, preventing measurement of modern $\delta^{18}O_{sp}$ values. After correcting the $\delta^{18}O_{sp}$ for the vital effect and isotope fractionation between calcite and water at 4 °C, the reconstructed $\delta^{18}O_{lw}$ ranges between −12.8 and −10.6 ‰ VSMOW. Mean $\delta^{18}O_{lw}$ is −11.5 ‰ VSMOW (SD = 0.4 ‰) for the entire record (Fig. 5). The reconstructed oxygen isotope value in the top sample (−11.3 ‰) is consistent with the modern $\delta^{18}O_{lw}$ range (−11.1 ‰ to −10.4 ‰) for 2019 and 2020.

Discussion

Major factors influencing the $\delta^{18}O$ signal at Lake Allos

The $\delta^{18}O$ signal in lake carbonates is primarily a function of the lake water oxygen isotope composition and water temperature (Stuiver, 1970; Leng and Marshall, 2004). The lake water oxygen isotope composition itself is a product of (i) the $\delta^{18}O$ value of the seawater from which it originally derived; (ii) rain-out history, seasonality and air-mass trajectory; and (iii) oxygen isotope fractionation of lake water compared to mean meteoric precipitation, primarily by evaporation but also by groundwater flux (Develle *et al.*, 2010; Roberts *et al.*, 2010). According to the modern oxygen isotope composition of Lake Allos' waters, $\delta^{18}O_{lw}$ plots along the global meteoric water line, showing no effect of evaporation after the summer season (Fig. 3). $\delta^{18}O$ in precipitation entering the lake varies according to the season, due to changes in air temperatures and differential contribution in vapor of Atlantic and Mediterranean origin. Therefore, a lowering in $\delta^{18}O_{lw}$ is expected to reflect an increasing contribution of water inflow from snowmelt, a higher contribution of precipitation of Atlantic origin, and/or precipitation occurring primarily during colder seasons (Celle-Jeanton *et al.*, 2004). In contrast, increasing $\delta^{18}O_{lw}$ is interpreted as a higher contribution of water inflow from rain versus snowmelt preferentially of Mediterranean origin and/or precipitation occurring mainly during warmer periods. In the catchment area, sources of signal change are evapotranspiration by vegetation, water losses by percolation into soils and delayed flows (stored in the ice, snow or soils). However, the $\delta^{18}O$ value of waters having percolated into soils might be considered as the average $\delta^{18}O$ value of local rainfall over several months (McDonnell

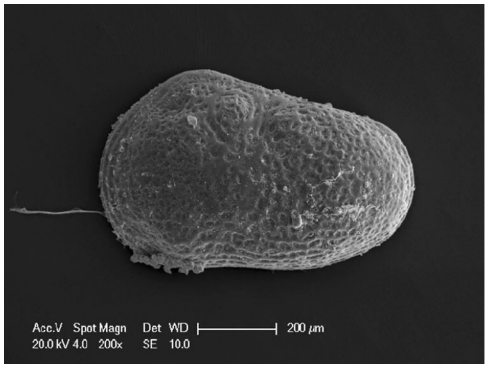

Figure 4. Scanning electron micrograph of a valve of *Cytherissa lacustris* (Aix-Marseille University, Saint Charles).

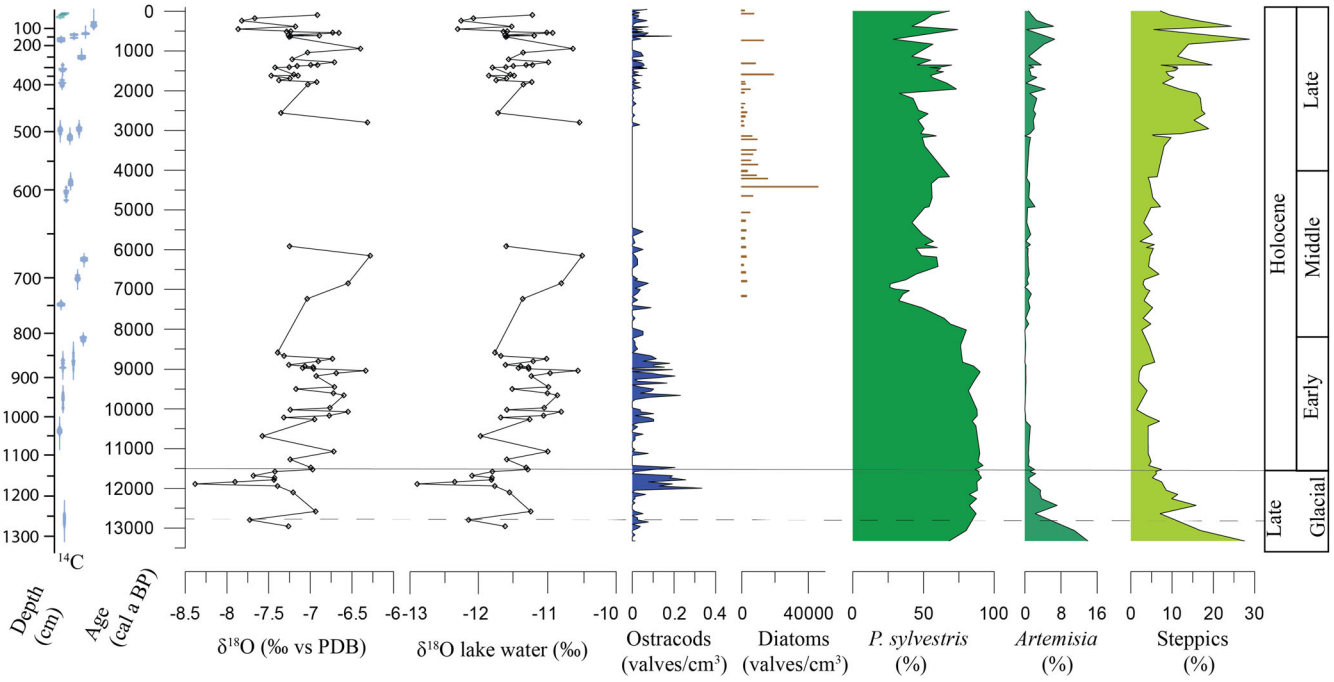

Figure 5. Oxygen isotope ratios (δ^{18}O) in ostracods (in ‰ VPDB) and lake water (δ$^{18}O_{lw}$ in ‰ VSMOW, the blue dashed line represents average modern δ$^{18}O_{lw}$ calculated from the three samples available) according to ages, concentrations in ostracods and diatoms (valves cm^{-3}), percentages of pollen of *P. sylvestris*, *Artemisia* sp. and the sum of steppics (*Artemisia*, Chenopodiaceae, Caryophyllaceae) from Cartier *et al.* (2018). The dashed line represents the onset of the Younger Dryas (YD) based on the oldest ^{14}C date and the black line represents the end of the YD according to ages and the pollen diagram, together with worldwide accepted limits for the Lateglacial and Holocene periods (Walker *et al.*, 2018). [Color figure can be viewed at wileyonlinelibrary.com]

et al., 1991; Tang and Feng, 2001). At Lake Allos, a low but permanent flow of water currently persists from the remains of a rock glacier. Four phases of glacial advances have been identified in the Allos watershed (Jorda, 1975; de Beaulieu and Jorda, 1977). Stages 1 and 2 (respectively at 1850–1900 and 2265 m a.s.l) pre-date the formation of Lake Allos and are attributed to the early Lateglacial (Brisset *et al.*, 2014). Stage 3, located at 2310 m a.s.l., is attributed to the YD, indicating a glacier advance near Lake Allos during this period (Brisset *et al.*, 2014). Finally, stage 4 is attributed to the last cooling period during the Late Holocene that might be related to the Neoglacial period (4500 cal a BP) or the LIA (Jorda, 1975; Brisset *et al.*, 2014).

The comparison between the δ$^{18}O_{lw}$ signal, vegetation evolution and the potential presence of a glacier, in particular during the YD, provides additional clues to identify factors influencing oxygen isotope variability. The marked drop in δ$^{18}O_{lw}$ ca. 12 000 cal a BP (2σ error = 360) probably occurred during the second half of the YD. Pollen analysis shows the presence of open vegetation from the base of the record to 1150 cm depth (ca. 11 700 cal a BP). A high percentage (30 %) of steppic taxa is consistent with the dominance of runoff processes in a sandur-type outwash plain at the glacier snout during massive deglaciation of the Allos cirque. Then, steppic taxa (*Artemisia*, Chenopodiaceae, Caryophyllaceae) increased again during the YD (Fig. 5). A similar vegetation is recorded during the YD in other paleoenvironmental studies of the Mediterranean Alps (de Beaulieu, 1977; Finsinger and Ribolini, 2001; Ponel *et al.*, 2001; Gandouin and Franquet, 2002). It is difficult to precisely define the onset of the YD based solely on the pollen diagram as steppic taxa progressively decrease from the base of the record. Nevertheless, the end of the YD probably corresponds to the end of the *Artemisia* period, associated with a decrease in steppic taxa and the extension of tree cover (black line on Fig. 5).

Other studies, such as the study of Lake Mondsee sediments in the north-eastern Alps, have shown that cooling at the onset of the YD is simultaneously reflected in ostracod δ^{18}O and vegetation (Lauterbach *et al.*, 2011). A similar synchronicity in the response of isotope and vegetation records is shown in a European synthesis by Reinig *et al.* (2021), recording the onset of the YD at 12 800 cal a BP (130 years earlier than thought). Therefore, the later drop in δ^{18}O values observed at Allos (ca. 12 000 cal a BP) could be related to the influence of a local glacier in the watershed rather than temperatures, at least during the YD interval. Following this hypothesis, an increasing glacier/snowmelt contribution could explain decreases in δ$^{18}O_{lw}$ when the presence of a glacier is suspected. During the mid-Holocene, vegetation starts to be highly influenced by humans, leading to an opening up of forests at lower altitudes, which limits the use of cross-comparison with the δ^{18}O signal (Cartier *et al.*, 2018; Figure 5). However, it can be seen that intervals with low δ$^{18}O_{lw}$ values during the Late Holocene and in particular during the LIA correspond to occurrences of *Ephedra* sp., supporting the presence of cooler periods (Cartier *et al.*, 2018).

Paleohydrology in the Mediterranean Alps and comparison with other climate reconstructions

Beginning of lake infilling and the climate reversal of the YD (i.e. from 13 350 to 11 500 cal a BP)

The first period of lake infilling of Lake Allos (13 350–12 700 cal a BP) can be attributed to the end of the Allerød considering the oldest ^{14}C date, giving an age of 13 070–12 800 cal a BP (2σ) at 1260 cm depth. As only one ^{14}C date predates the onset of the YD, uncertainties remain regarding the chronology but climatic conditions must necessarily have been relatively warmer than previous periods to allow the massive deglaciation of the cirque of Allos. Additional

information can be obtained from the pollen diagram, which documents an open landscape characteristic of the pre-Holocene period from the base of the record to 1150 cm depth (ca. 11 700 cal a BP; min: 11 570, max: 11 920; 95 %) (Fig. 5). The corresponding age for this depth is consistent with recognized boundaries of the YD, i.e. 12 800–11 500 cal a BP from the Greenland ice-core (GS-1) and mid-European isotope records (Reinig *et al.*, 2021) (Fig. 6).

In the Northern Alps, the $\delta^{18}O$ record of lake Leysin (1255 m a.s.l., Switzerland), Schwander *et al.*, 2000) shows quasi-simultaneous temperature changes between Greenland and Europe during the YD. Records from the northern Alps or its foreland display consistent shapes of the YD, similar to the Ammersee record (533 m a.s.l.) (Fig. 6). In addition, oxygen isotope records from Lake Mondsee (481 m a.s.l., Lauterbach *et al.*, 2011), Lake Gerzensee (603 m a.s.l., von Grafenstein *et al.*, 2013), Hölloch cave (700 m a.s.l., Li *et al.*, 2021) and the TEX86 temperature record from Lake Lucerne (434 m a.s.l., Blaga *et al.*, 2013) also document synchronous changes during the YD.

Located at higher altitudes, the $\delta^{18}O_{lw}$ record from Lake Allos (2230 m a.s.l.) in the Southern French Alps clearly differs from those documented in the Northern Alps. According to the age–depth model, the beginning of the YD is marked by relatively high $\delta^{18}O$ values compared to the second half of the YD (ca. after 12 000 cal a BP; Fig. 5). Several hypotheses might explain the persistence of high $\delta^{18}O$ values during this period, including (i) water storage induced by the presence of a local glacier in the watershed, (ii) a lower temperature shift at the Allerød–YD transition in the Southern French Alps and (iii) a greater influence of precipitation of Mediterranean origin to counteract a large cooling. Several factors could also have played a simultaneous role in the changes observed. The first hypothesis, i.e. water storage induced by the presence of a glacier, agrees with datings of moraines in the Southern French Alps (Darnault *et al.*, 2012; Figure 6). A meltwater flux during summer is not excluded but was probably of less importance to the lake budget than during the second half of the YD. Concerning a lower temperature shift (hypothesis 2), the study of paleo-extents of the Argentière glacier close to the study site

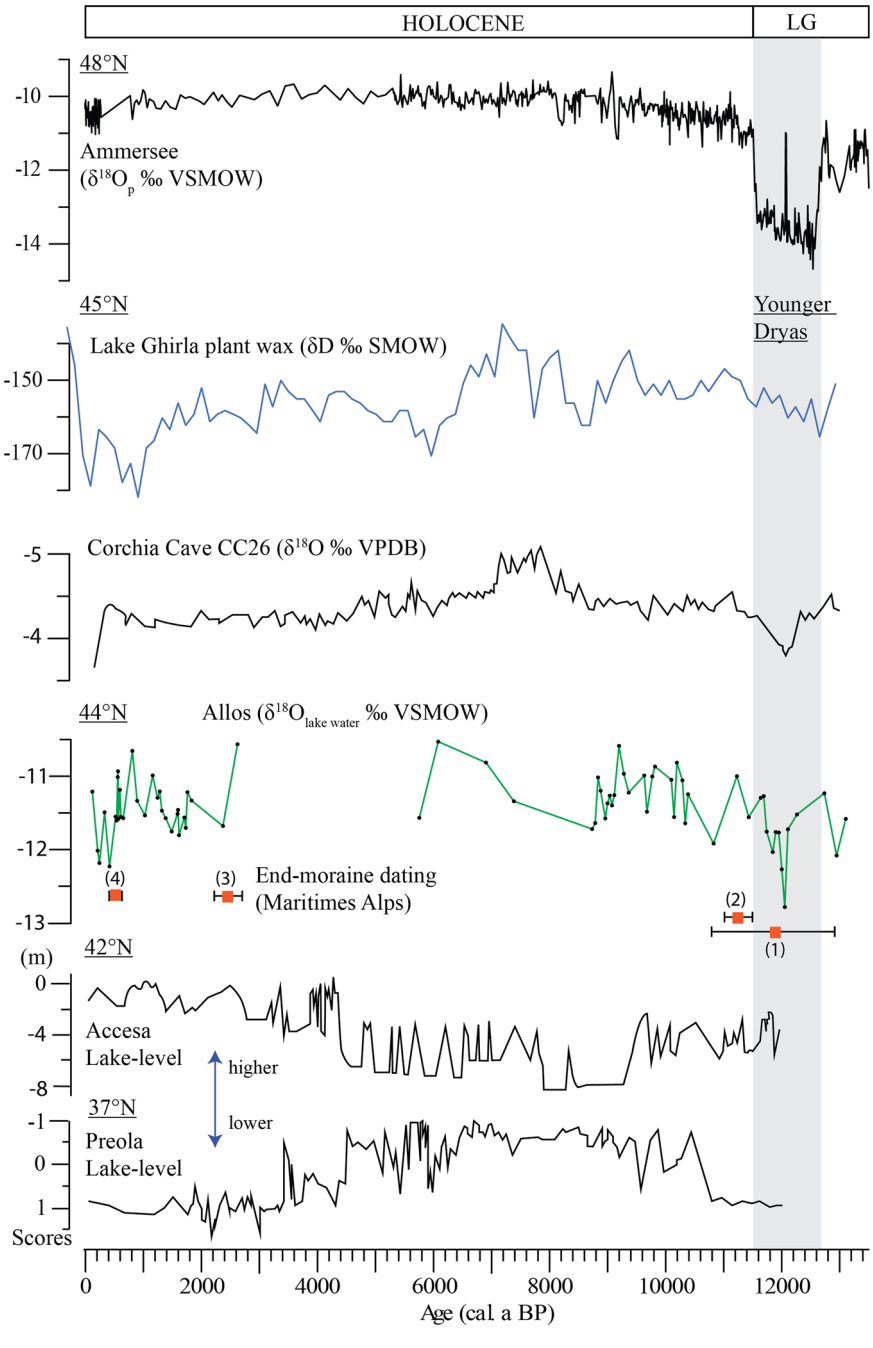

Figure 6. Estimated $\delta^{18}O$ ($\delta^{18}O_{lw}$, ‰ VSMOW) in the lake waters of Lake Allos compared to other records: oxygen isotope ratios in precipitation ($\delta^{18}O_p$, ‰ VSMOW) based on the record of Lake Ammersee (Germany; von Grafenstein *et al.*, 1999); Lake Ghirla plant wax (δD, ‰ SMOW) at the foot of the Southern Alps (Wirth and Sessions, 2016); oxygen isotope record ($\delta^{18}O$, ‰ VPDB) of Corchia Cave CC26 (Northern Italy; Zanchetta *et al.*, 2007); lake-level fluctuations (m) at Accesa (Italy; Magny *et al.*, 2007); lake level reconstruction at Preola (Southern Italy; Magny *et al.*, 2011). Locations of the sites are shown on Fig. 1. Ages of end-moraine and polished bedrock (Maritime Alps) dated by ^{10}Be and ^{14}C methods are from: (1) Spagnolo and Ribolini (2019); (2) Darnault *et al.* (2012); (3) Federici *et al.* (2008); (4) Ribolini *et al.* (2007); and (5) Federici and Stefanini (2001). [Color figure can be viewed at wileyonlinelibrary.com]

(Protin *et al.*, 2019) invalidates this hypothesis as reconstructed temperature shifts (ΔT varying between 3.6 and 5.5 °C compared to modern temperatures) are in the same range as temperature reconstructions from the Northern Alps (e.g. ΔT of 3.9 °C at the YD–Holocene transition in the Swiss Alps; Samartin *et al.*, 2012). Finally, the third hypothesis (a higher influence of precipitation of Mediterranean origin) is in accordance with the hydrogen isotope record of plant waxes from Lake Ghirla in the Southern Alps showing unexpectedly high δD_{wax} values during the YD (Wirth and Sessions, 2016). This signal was interpreted as a shift from a northern North Atlantic to a southern North Atlantic/western Mediterranean Sea source due to a southward migration of the westerlies with climate cooling. Assuming a temperature shift (YD–modern conditions) varying between 3.6 and 5.5 °C (Protin *et al.*, 2019), an altitudinal effect of −0.2 ‰ per 100 m (e.g. Schürch *et al.*, 2003) and a correlation between $\delta^{18}O$ in precipitation and air temperatures of 0.33 ‰ per °C (Draix station; $r^2 = 0.54$; Supporting Information Fig. S1), the precipitation reaching Allos at the beginning of the YD may have been the result of a mixture of 50 % Atlantic – 50 % Mediterranean (30 % / 70 %, respectively) to counteract the effect of cooling on the $\delta^{18}O$ record.

At a broader scale, a higher contribution of Mediterranean precipitation in the Southern French Alps would fit a recent study published in Rea *et al.* (2020) based on glacier, pollen and chironomid assemblages, showing that the YD was certainly characterized by the presence of a positive Scandinavia (SCAND) climate configuration pushing storm tracks south and east. To summarize, while the temperature hypothesis can be excluded, glacier storage and a Mediterranean precipitation source remain plausible explanations for high $\delta^{18}O$ values during this period.

During the second half of the YD, the isotopic record of Lake Allos also presents an original shape. The $\delta^{18}O$ record is marked by a sharp drop to low $\delta^{18}O$ values corresponding to the lowest values of the record (−12.8 ‰ VSMOW) ca. 12 000 cal a BP. These changes are probably the result of large freshwater inputs to the lake due to glacier melting. This implies a large influence of glacier dynamics in the watershed on the isotopic signal, as suggested by the comparison with the pollen diagram. Alternatively, the presence of humid conditions would fit the regional geomorphological studies from the Maritime Alps, indicating the presence of glacier advances ca. 12 500–12 300 cal a BP (Pauly *et al.*, 2018; Spagnolo and Ribolini, 2019).

The Holocene period from 11 500 cal a BP to the present day

Isotope records covering the transition from the Lateglacial to the Holocene are very sparse in the Alps, and almost non-existent in the Southern French Alps. A moraine dating to the Preboreal period in the Maritime Alps (Fig. 6; Federici *et al.*, 2008) suggests new glacial advances at the beginning of the Holocene. Although supported by only a few samples, a drop in $\delta^{18}O_{lw}$ in the record of Allos (from −11 to −12 ‰ VSMOW) ca. 10 800 cal a BP seems to follow the cold and humid Preboreal oscillation ca. 11 300 cal a BP (Ilyashuk *et al.*, 2009).

Between 9800 and 8400 cal a BP, $\delta^{18}O_{lw}$ at Lake Allos increased, reaching a maximum of −10.7 ‰ VSMOW, and then decreased to −11.8 ‰ VSMOW. The millennial-scale change in the $\delta^{18}O$ values is assumed to be related primarily to changes in air temperature and precipitation regime rather than to glacier influence. To the best of our current knowledge (Brisset *et al.*, 2014, 2015), it seems unlikely that the upper moraines date back to this time interval in the watershed of Allos; however, remaining moraines not yet sampled are under investigation. Increasing $\delta^{18}O$ values might then be the result of a higher contribution of precipitation occurring during warmer seasons and/or preferentially of Mediterranean origin. Indeed, the Early Holocene in the northern mid-latitudes is characterized by the highest summer and lowest winter solar insolation (Laskar *et al.*, 2004). Therefore, higher summer temperatures are recorded in the Eastern Alps (Ilyashuk *et al.*, 2011). In the Southern Alps, a high-resolution $\delta^{13}C$ isotopic signal highlights an early Holocene warming and/or a climate oscillation called the '9.3 ka' dry climate event (Audiard *et al.*, 2021).

In contrast, the period 9200–8400 cal a BP suggests a higher contribution of snowmelt, precipitation of Atlantic origin and/or the presence of colder conditions. More broadly, the northwestern Mediterranean region at the beginning of the Holocene generally experienced a long-term trend towards humid conditions from 9200 to 6800 cal a BP, as evidenced in lake isotope records (Roberts *et al.*, 2008), caves (Rio Martino and Corchia Cave, Regattieri *et al.*, 2019 and Zanchetta *et al.* 2007) and lake level reconstructions (Harrison and Digerfeldt, 1993; Jalut *et al.*, 2009; Magny *et al.*, 2013) (Fig. 6).

At the transition from the Early to Mid-Holocene (8200 cal a BP), low data resolution limits our ability to assess fine variations in the $\delta^{18}O$ record. However, we observe a general trend towards increasing $\delta^{18}O_{lw}$ culminating ca. 6100 cal a BP, representing the highest value of the sequence (−10.6 ‰ VSMOW), followed by an abrupt decrease at 5700 cal a BP, unfortunately supported by only one data point. During that time period, precipitation reconstruction (Brayshaw *et al.*, 2011) and paleoclimate data from lake isotope records (Roberts *et al.*, 2011) indicate drier conditions from 8000 to 6000 cal a BP in both Western and Eastern Mediterranean regions. This period also represents a thermal optimum in the Northern Hemisphere between 30 and 60°N (Kaufman *et al.*, 2020).

For the last 2800 cal a BP, our results suggest major paleohydrological changes near Lake Allos. A shift from high $\delta^{18}O_{lw}$ to low $\delta^{18}O$ at 2300 cal a BP is concomitant with increasing torrential activity at Lake Allos (Brisset *et al.*, 2017) and in the Southern French Alps during the Iron Age time interval interpreted as a cooler and more humid period (Jorda, 1992; Sivan *et al.*, 2006); however, the low resolution limits further interpretation (Fig. 7). Then, at the beginning of the Roman Period ca. 1900–1800 cal a BP, higher $\delta^{18}O_{lw}$ suggests the presence of higher air temperatures and/or a higher contribution of rain to the lake (versus snowmelt) preferentially of Mediterranean origin. A drier period at lower altitudes in the valleys is illustrated by human occupation closer to or within current riverbeds (Bravard *et al.*, 1992; Jorda, 1992). From 1800 to 1300 cal a BP, low $\delta^{18}O_{lw}$ values suggest lower air temperatures and/or a higher contribution of precipitation (mostly snow) of Atlantic origin to the lake. The Late Antiquity also coincides with higher torrential activity both at high altitude at Allos (Brisset *et al.*, 2017) and in lowlands (Sivan *et al.*, 2006), negative temperature anomalies in tree ring records (Büntgen and Tegel, 2011) and glacier advances in the European Alps (Holzhauser *et al.*, 2005) (Fig. 7). Higher $\delta^{18}O_{lw}$ occurs again from 1300 to 500 cal a BP, which might correspond to the MCA also seen in the tree ring record of Corona *et al.* (2011) (Fig. 7). Regarding our results, the MCA shows several oscillations in the $\delta^{18}O$ record with three peaks ca. 1200, 850 and 600 cal a BP. The transition between the MCA and LIA at 500 cal a BP is very sharp with $\delta^{18}O_{lw}$ highly depleted during two low excursions. These $\delta^{18}O$ values are similar to the values obtained in the second part of the YD. This abrupt decrease might be explained by lower air

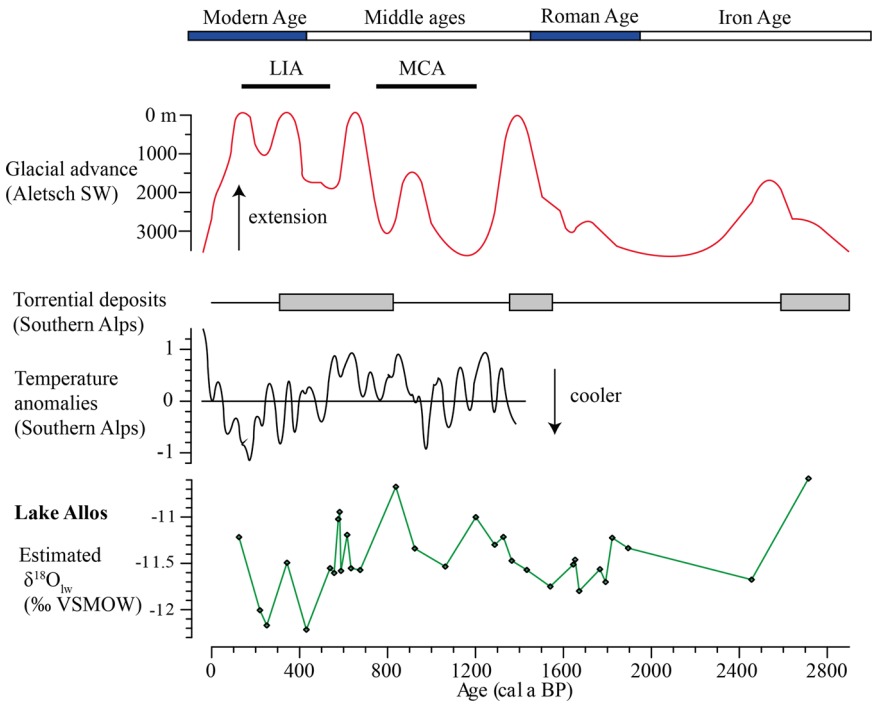

Figure 7. Estimated $\delta^{18}O$ ($\delta^{18}O_{lw}$, ‰ VSMOW) in Allos' lake waters for the last 3000 years compared to global signatures of the Medieval Climate Anomaly (MCA) and Little Ice Age (LIA) (Mann *et al.*, 2009), glacial advances at Aletsch in Switzerland (Holzhauser *et al.*, 2005), torrential deposits in Southern French Alps (Sivan *et al.*, 2006) and temperature anomalies reconstructed from dendrochronological data (Corona *et al.*, 2011). [Color figure can be viewed at wileyonlinelibrary.com]

temperatures and/or higher freshwater inputs from snowmelt to the lake preferentially of Atlantic origin. During the LIA, sedimentological studies show increasing fluvial activity in the Southern French Alps, at Allos (Wilhelm *et al.*, 2012; Brisset *et al.*, 2017) and downstream (Miramont *et al.*, 1998; Sivan *et al.*, 2006), a water level rise in the Jura (Magny *et al.*, 2001), and glacial tongue advances in both the Northern and Southern Alps (Holzhauser *et al.*, 2005; Ivy-Ochs *et al.*, 2009; Figure 7). Overall, two moraines in the Maritime Alps showing glacial advances during the Iron Age ca. 2400 cal a BP (Ribolini *et al.* (2007) and the LIA ca. 450 cal a BP (Federici and Stefanini, 2001) are coherent with low $\delta^{18}O$ values at Allos (Fig. 6). The fourth stage of glacial advance at Allos described in Jorda (1975) could then be linked to the LIA given the intensity of the event in the $\delta^{18}O$ record. However, the sequence discontinuity and low periodic resolution require further isotopic studies for the Mediterranean Alps.

Finally, comparing oxygen isotope records from Northern-mid and Southern Europe (Fig. 6) with the $\delta^{18}O$ record at Lake Allos allows a better understanding of how air temperatures and hydrology have responded to climate change during the end of the Lateglacial and Holocene periods. The record of Allos shows an alternation of glacier growth and melting during the YD and a general high variability in freshwater inputs (as in Bakke *et al.*, 2009) while air temperature proxies (von Grafenstein *et al.*, 1999; Schwander *et al.*, 2000) show similar boundaries with Greenland ice cores. During the Holocene, the record of Lake Allos highlights a general trend towards drier conditions from the Early to mid-Holocene (ca. 6000 cal a BP) followed by wetter conditions from 2800 cal a BP to the present day. Unfortunately, the resolution of the record prevents further interpretations for the mid-Holocene, and other events might have occurred (see Cartier *et al.*, 2019). This trend is the opposite of lake water level variations in Southern Europe recorded at Lake Preola in Southern Italy (Magny *et al.*, 2011; Figure 6) but in agreement with local lake water level reconstructions (Harrison *et al.*, 1993; Digerfeldt *et al.*, 1997) and isotope cave records (Regattieri *et al.*, 2019). Whereas changes in global air temperatures in the Northern Hemisphere were relatively smooth during the Holocene with a progressive increase in air temperatures until 6000 cal a BP followed by a decreasing trend until the 19th century (Kaufman *et al.*, 2020), local hydroclimate records from the Mediterranean Alps show a higher variability with centennial and millennial climate oscillations.

Conclusions

Sediments from Lake Allos have allowed for the analysis of oxygen isotope ratios in valves of *Cytherissa lacustris*, a species encountered in deep lakes. Variation in $\delta^{18}O$ covers the end of the Lateglacial and the Holocene (except from 5800 to 2800 cal a BP). $\delta^{18}O_{lw}$ was estimated after correcting ostracod $\delta^{18}O$ values with the vital effect of *C. lacustris* and the effect of isotope fractionation at equilibrium between calcite and water at 4 °C. The main factors influencing the isotopic record are estimated to be: variation in air temperatures, freshwater inputs through melting glacier/snowmelt contribution, and meteoric precipitation sources (West from the Atlantic and South from the Mediterranean region). Despite only one ^{14}C date before the Holocene, our data indicate the persistence of a steppic vegetation during the YD. Relatively high $\delta^{18}O_{lw}$ values at that time could be related to glacier water storage and Mediterranean precipitation source. Then, during the second half of the YD, the large drop in $\delta^{18}O_{lw}$ might be the result of higher freshwater inputs to the lake budget. During the Holocene, the highest $\delta^{18}O_{lw}$ value of the record was reached ca. 6100 cal a BP during a thermal optimum at this latitude, suggesting a potential role of climate in large vegetation succession in the Southern French Alps. Finally, the Late Holocene (from 2800 cal a BP to the present day) shows several oscillations in $\delta^{18}O_{lw}$ following major climate phases recognized at the European scale and glacier advances/retreat in the Western Alps: a higher contribution of ice/snowmelt inputs to the lake and/or lower temperatures during the Late Antiquity and LIA and a reverse trend during the Roman Warm Period and MCA. Therefore, the fourth stage of glacial advance in the watershed of Allos could be linked to the LIA given the intensity of the event in the $\delta^{18}O$ record. However, new studies on hydroclimate in high-altitude environments are required to fully understand these questions due to the discontinuity of the sequence.

Supporting information

Additional supporting information can be found in the online version of this article.This article includes online-only Supplemental Data.

Acknowledgements. We thank C. Vallet-Coulomb (CEREGE, France) and the British Geological Survey (UK) for the oxygen isotope analysis of modern waters. Thanks go to D. Sabatier (CEREGE, France) for providing material for picking ostracods and to H. Bruneton for her valuable help with ostracod determination. Many thanks to O. Laurent and M.-F. Leccia from the National Park of Mercantour for their support and sampling of modern waters. Thanks to R. Pickering for rereading the manuscript. The PhD thesis of R. Cartier (Aix-Marseille University) was funded by the 'Ministère de l'Enseignement Supérieur, de la Recherche et de l'Innovation'. Several projects supported the research work: Programme d'Intérêt Transfrontalier (Parc National du Mercantour, France) led by F. Suméra (SRA-PACA) entitled 'Etude de l'usage et de l'occupation du sol et du territoire Mercantour', and the project LADICIA, 'Quand l'homme et le climat façonnent la montagne méridionale: le Lac d'Allos, une histoire du Détritisme, des Instabilités Climatiques et des Impacts Anthropiques' (Région PACA, ref. 2010_08_012) led by C. Miramont (IMBE).

Abbreviations. LIA, Little Ice Age; MCA, Medieval Climate Anomaly; NAO, North Atlantic Oscillation; YD, Younger Dryas..

References

Arnaud F, Poulenard J, Giguet-Covex C *et al.* 2016. Erosion under climate and human pressures: an alpine lake sediment perspective. *Quaternary Science Reviews* **152**: 1–18. https://doi.org/10.1016/j.quascirev.2016.09.018

Audiard B, Ricci G, Porraz G *et al.* 2021 Identifying Short-Term Climatic Changes Through Isotopic Charcoal Analyses Early Holocene Warming and the '9.3 Ky' Event at the Mesolithic Site of la Baume de Monthiver (Var, France). https://hal.archives-ouvertes.fr/hal-03455722

Auer I, Böhm R, Jurkovic A *et al.* 2007. HISTALP – historical instrumental climatological surface time series of the Greater Alpine Region. *International Journal of Climatology* **27**: 17–46. https://doi.org/10.1002/joc.1377

Bakke J, Lie Ø, Heegaard E *et al.* 2009. Rapid oceanic and atmospheric changes during the Younger Dryas cold period. *Nature Geoscience* **2**: 202–205. https://doi.org/10.1038/ngeo439

de Beaulieu J, Jorda M. (1977). Tardiglaciaire et postglaciaire des Alpes de Haute-Provence. Le glaciaire de la Blanche, Trois évêchés. *Quaternaire*, **14**(3), 3-15.

Blaga CI, Reichart G-J, Lotter AF *et al.* 2013. A TEX 86 lake record suggests simultaneous shifts in temperature in Central Europe and Greenland during the last deglaciation. *Geophysical Research Letters* **40**: 948–953. https://doi.org/10.1002/grl.50181

Blenckner T, Adrian R, Livingstone DM *et al.* 2007. Large-scale climatic signatures in lakes across Europe: A meta-analysis. *Global Change Biology* **13**: 1314–1326. https://doi.org/10.1111/j.1365-2486.2007.01364.x

Bolle H-J (ed). 2003. *Mediterranean Climate.* Springer: Berlin.

Bravard J-P, Verot-Bourrely A, Salvador P-G. 1992. Le climat d'après les informations fournies par les enregistrements sédimentaires fluviatilis étudiés sur des sites archéologiques. Nouvelles de l'archéologie. Paper presented at the Round Table, Le climat à la fin de l'Age du Fer et dans l'Antiquité (500 BC-500 AD): méthodes d'approche et résultats. Epona: 7–13.

Brayshaw DJ, Rambeau CMC, Smith SJ. 2011. Changes in Mediterranean climate during the Holocene: insights from global and regional climate modelling. *Holocene.* **21**: 15–31. https://doi.org/10.1177/0959683610377528

Brisset E, Guiter F, Miramont C *et al.* 2015. Lateglacial/Holocene environmental changes in the Mediterranean Alps inferred from lacustrine sediments. *Quaternary Science Reviews* **110**: 49–71. https://doi.org/10.1016/j.quascirev.2014.12.004

Brisset E, Guiter F, Miramont C *et al.* 2017. The overlooked human influence in historic and prehistoric floods in the European Alps. *Geology* **45**: 347–350. https://doi.org/10.1130/G38498.1

Brisset E, Miramont C, Guiter F *et al.* 2014. Données nouvelles sur la chronologie de la déglaciation dans la vallée du Haut-Verdon (lac d'Allos, Alpes françaises du Sud). Quaternaire. *Revue de l'Association française pour l'étude du Quaternaire* **25/2**: 147–156.

Büntgen U, Tegel W. 2011. European tree-ring data and the Medieval Climate Anomaly. *PAGES News* **19**: 14–15. https://doi.org/10.22498/pages.19.1.14

Caporaletti M. 2011. Ostracods and stable isotopes: proxies for palaeoenvironmental reconstructions. *Joannea--Geologie und Palaontologie* **11**: 345–359 [PubMed: 28123353].

Cartier R, Brisset E, Guiter F *et al.* 2018. Multiproxy analyses of Lake Allos reveal synchronicity and divergence in geosystem dynamics during the Lateglacial/Holocene in the Alps. *Quaternary Science Reviews* **186**: 60–77. https://doi.org/10.1016/j.quascirev.2018.02.016

Cartier R, Sylvestre F, Paillès C *et al.* 2019. Diatom-oxygen isotope record from high-altitude Lake Petit (2200 m a.s.l.) in the Mediterranean Alps: shedding light on a climatic pulse at 4.2 ka. *Climate of the Past* **15**: 253–263. https://doi.org/10.5194/cp-15-253-2019

Carzon J. 1958. Monographie hydrologique du Verdon. *Houille Blanche* **44**: 717–728. https://doi.org/10.1051/lhb/1958011

Celle-Jeanton H, Gonfiantini R, Travi Y *et al.* 2004. Oxygen-18 variations of rainwater during precipitation: application of the Rayleigh model to selected rainfalls in Southern France. *Journal of Hydrology* **289**: 165–177. https://doi.org/10.1016/j.jhydrol.2003.11.017

Coplen TB. 2007. Calibration of the calcite–water oxygen-isotope geothermometer at Devils Hole, Nevada, a natural laboratory. *Geochimica et Cosmochimica Acta* **71**: 3948–3957. https://doi.org/10.1016/j.gca.2007.05.028

Coplen TB, Kendall C, Hopple J. 1983. Comparison of stable isotope reference samples. *Nature* **302**: 236–238. https://doi.org/10.1038/302236a0

Corona C, Edouard J-L, Guibal F *et al.* 2011. Long-term summer (AD 751–2008) temperature fluctuation in the French Alps based on tree-ring data. *Boreas* **40**: 351–366. https://doi.org/10.1111/j.1502-3885.2010.00185.x

Cramer W, Guiot J, Fader M *et al.* 2018. Climate change and interconnected risks to sustainable development in the Mediterranean. *Nature Climate Change* **8**: 972–980. https://doi.org/10.1038/s41558-018-0299-2

Darnault R, Rolland Y, Braucher R *et al.* 2012. Timing of the last deglaciation revealed by receding glaciers at the Alpine-scale: impact on mountain geomorphology. *Quaternary Science Reviews* **31**: 127–142. https://doi.org/10.1016/j.quascirev.2011.10.019

Decrouya L, Vennemanna WT, Arizteguib D. (2011). Controls on ostracod valve geochemistry: Part 2. Carbon and oxygen isotope compositions. *Geochimica et Cosmochimica Acta*, **75**(22), 7380-7399.

de Beaulieu JL. 1977. Contribution pollenanalytique à l'histoire tardiglaciaire et holocène de la végétation des Alpes méridionales françaises. *Centre régional de documentation pédagogique. Unpublished Doctoral Thesis, Université d'Aix-Marseille-3, 358.*

Develle AL, Herreros J, Vidal L *et al.* 2010. Controlling factors on a paleo-lake oxygen isotope record (Yammoûneh, Lebanon) since the Last Glacial Maximum. *Quaternary Science Reviews* **29**: 865–886. https://doi.org/10.1016/j.quascirev.2009.12.005

Devriendt LS, McGregor HV, Chivas AR. 2017. Ostracod calcite records the $^{18}O/^{16}O$ ratio of the bicarbonate and carbonate ions in water. *Geochimica et Cosmochimica Acta* **214**: 30–50. https://doi.org/10.1016/j.gca.2017.06.044

Digerfeldt G, de Beaulieu J-L, Guiot J *et al.* 1997. Reconstruction and paleoclimatic interpretation of Holocene lake-level changes in Lac de Saint-Léger, Haute-Provence, southeast France. *Palaeogeography, Palaeoclimatology, Palaeoecology* **136**: 231–258. https://doi.org/10.1016/S0031-0182(97)00075-8

Drysdale R, Zanchetta G, Hellstrom J *et al.* 2006. Late Holocene drought responsible for the collapse of Old World civilizations is recorded in an Italian cave flowstone. *Geology* **34**: 101–104. https://doi.org/10.1130/G22103.1

Durand Y, Giraud G, Laternser M *et al.* 2009a. Reanalysis of 47 years of climate in the French Alps (1958–2005): climatology and trends for snow cover. *Journal of Applied Meteorology and Climatology* **48**: 2487–2512. https://doi.org/10.1175/2009JAMC1810.1

Durand Y, Laternser M, Giraud G *et al.* 2009b. Reanalysis of 44 yr of climate in the French Alps (1958–2002): methodology, model validation, climatology, and trends for air temperature and precipitation. *Journal of Applied Meteorology and Climatology* **48**: 429–449. https://doi.org/10.1175/2008JAMC1808.1

Etienne D, Wilhelm B, Sabatier P *et al.* 2013. Influence of sample location and livestock numbers on Sporormiella concentrations and accumulation rates in surface sediments of Lake Allos, French Alps. *Journal of Paleolimnology* **49**: 117–127. https://doi.org/10.1007/s10933-012-9646-x

Federici PR, Granger DE, Pappalardo M *et al.* 2008. Exposure age dating and Equilibrium Line Altitude reconstruction of an Egesen moraine in the Maritime Alps, Italy. *Boreas* **37**: 245–253. https://doi.org/10.1111/j.1502-3885.2007.00018.x

Federici PR, Ribolini A, Spagnolo M. 2017. Glacial history of the Maritime Alps from the Last Glacial Maximum to the little ice age. *Geological Society, London, Special Publications* **433**: 137–159. https://doi.org/10.1144/SP433.9

Federici PR, Stefanini MC. 2001. Abhandlungen-Evidence and chronology of the Little Ice Age in the Argentera Massif (Italian maritime alps). *Zeitschrift für Gletscherkunde und Glazialgeologie* **37**: 35–48.

Finsinger W, Ribolini A 2001 Late Glacial to Holocene Deglaciation of the Colle Del Vei Del Bouc-Colle Del Sabbione Area (Argentera Massif, Maritime Alps, Italy-France). *Geografia Fisica e Dinamica Quaternaria24: 141-156.*

Friedman I, O'Neil JR. (1977). *Compilation of stable isotope fractionation factors of geochemical interest* (Vol. **440**). US Government Printing Office.

Gandouin E, Franquet E. 2002. Late Glacial and Holocene chironomid assemblages in Lac Long Inférieur (southern France, 2090 m): palaeoenvironmental and palaeoclimatic implications. *Journal of Paleolimnology* **28**: 317–328. https://doi.org/10.1023/A:1021690122999

Harrison SP, Digerfeldt G. 1993. European lakes as palaeohydrological and palaeoclimatic indicators. *Quaternary Science Reviews* **12**: 233–248. https://doi.org/10.1016/0277-3791(93)90079-2

Harrison SP, Prentice IC, Guiot J. 1993. Climatic controls on Holocene lake-level changes in Europe. *Climate Dynamics* **8**: 189–200. https://doi.org/10.1007/BF00207965

Holzhauser H, Magny M, Zumbuühl HJ. 2005. Glacier and lake-level variations in west-central Europe over the last 3500 years. *Holocene* **15**: 789–801. https://doi.org/10.1191/0959683605hl853ra

IAEA/WMO. 2019. Global network of isotopes in precipitation. The GNIP database. Accessible at: www.iaea.org/water.

Ilyashuk B, Gobet E, Heiri O *et al.* 2009. Lateglacial environmental and climatic changes at the Maloja Pass, Central Swiss Alps, as recorded by chironomids and pollen. *Quaternary Science Reviews* **28**: 1340–1353. https://doi.org/10.1016/j.quascirev.2009.01.007

Ilyashuk EA, Koinig KA, Heiri O *et al.* 2011. Holocene temperature variations at a high-altitude site in the Eastern Alps: a chironomid record from Schwarzsee ob Sölden, Austria. *Quaternary Science Reviews* **30**: 176–191. https://doi.org/10.1016/j.quascirev.2010.10.008 [PubMed: 21317974]

Ivy-Ochs S, Kerschner H, Maisch M *et al.* 2009. Latest Pleistocene and Holocene glacier variations in the European Alps. *Quaternary Science Reviews* **28**: 2137–2149. https://doi.org/10.1016/j.quascirev.2009.03.009

Jalut G, Dedoubat JJ, Fontugne M *et al.* 2009. Holocene circum-Mediterranean vegetation changes: climate forcing and human impact. *Quaternary International* **200**: 4–18. https://doi.org/10.1016/j.quaint.2008.03.012

Jorda M. 1975. Les montagnes du Haut Verdon, Etude géomorphologique. *Méditerranée* **20**: 37–58. https://doi.org/10.3406/medit.1975.1585

Jorda M. 1992 *Morphogenèse et fluctuations climatiques dans les Alpes françaises du Sud de l'Age du Bronze au haut Moyen Age. Nouvelles de l'archéologie*. Paper presented at the Round Table "Le climat à la fin de l'Age du Fer et dans l'Antiquité (500 BC-500 AD): méthodes d'approche et résultats." Epona, 14–20.

Kaufman D, McKay N, Routson C *et al.* 2020. Holocene global mean surface temperature, a multi-method reconstruction approach. *Scientific Data* **7**: 201. https://doi.org/10.1038/s41597-020-0530-7 [PubMed: 32606396]

Kim ST, O'Neil JR. 1997. Temperature dependence of ^{18}O. *Geochimica et Cosmochima Acta* **61** [PubMed: 34613475].

Laskar J, Robutel P, Joutel F *et al.* 2004. A long-term numerical solution for the insolation quantities of the Earth. *Astronomy and Astrophysics* **428**: 261–285. https://doi.org/10.1051/0004-6361:20041335

Lauterbach S, Brauer A, Andersen N *et al.* b 2011. Environmental responses to Lateglacial climatic fluctuations recorded in the sediments of pre-Alpine Lake Mondsee (northeastern Alps). *Journal of Quaternary Science* **26**: 253–267. https://doi.org/10.1002/jqs.1448.

Leng MJ, Marshall JD. 2004. Palaeoclimate interpretation of stable isotope data from lake sediment archives. *Quaternary Science Reviews* **23**: 811–831. https://doi.org/10.1016/j.quascirev.2003.06.012

Li H, Spötl C, Cheng H. 2021. A high-resolution speleothem proxy record of the Late Glacial in the European Alps: extending the NALPS19 record until the beginning of the Holocene. *Journal of Quaternary Science* **36**: 29–39. https://doi.org/10.1002/jqs.3255

Magny M, Combourieu-Nebout N, de Beaulieu JL *et al.* 2013. North–south palaeohydrological contrasts in the central Mediterranean during the Holocene: tentative synthesis and working hypotheses. *Climate of the Past* **9**: 2043–2071. https://doi.org/10.5194/cp-9-2043-2013

Magny M, de Beaulieu J-L, Drescher-Schneider R *et al.* 2007. Holocene climate changes in the central Mediterranean as recorded by lake-level fluctuations at Lake Accesa (Tuscany, Italy). *Quaternary Science Reviews* **26**: 1736–1758. https://doi.org/10.1016/j.quascirev.2007.04.014

Magny M, Guiot J, Schoellammer P. 2001. Quantitative reconstruction of Younger Dryas to mid-Holocene paleoclimates at le Locle, Swiss Jura, using pollen and lake-level data. *Quaternary Research* **56**: 170–180. https://doi.org/10.1006/qres.2001.2257

Magny M, Vannière B, Calo C *et al.* 2011. Holocene hydrological changes in south-western Mediterranean as recorded by lake-level fluctuations at Lago Preola, a coastal lake in southern Sicily, Italy. *Quaternary Science Reviews* **30**: 2459–2475. https://doi.org/10.1016/j.quascirev.2011.05.018

Mann ME, Zhang Z, Rutherford S. (2009). Global signatures and dynamical origins of the little ice age and medieval climate anomaly. *Science*, **326**(5957), 1256-1260.

McDonnell JJ, Stewart MK, Owens IF. 1991. Effect of catchment-scale subsurface mixing on stream isotopic response. *Water Resources Research* **27**: 3065–3073. https://doi.org/10.1029/91WR02025

Meisch C. 2000 *Freshwater Ostracoda of Western and Central Europe*. Spektrum Akademischer Verlag.

Miramont C, Jorda M, Pichard G. 1998. Évolution historique de la morphogenèse et de la dynamique fluviale d'une rivière méditerranéenne: l'exemple de la moyenne durance (France du sud-est). *Géographie Physique et Quaternaire* **52**: 381–392. https://doi.org/10.7202/004855ar

Morrison J, Brockwell T, Merren T *et al.* 2001. On-line high-precision stable hydrogen isotopic analyses on nanoliter water samples. *Analytical Chemistry* **73**: 3570–3575. https://doi.org/10.1021/ac001447t [PubMed: 11510820]

ONEMA. 2013. Annual monitoring of Lake of Allos. Available at: www.onema.fr/Bases-de-donnees.

Pauly M, Helle G, Miramont C *et al.* 2018. Subfossil trees suggest enhanced Mediterranean hydroclimate variability at the onset of the Younger Dryas. *Scientific Reports* **8**: 13980. https://doi.org/10.1038/s41598-018-32251-2[PubMed: 30228341]

Ponel P, Andrieu-Ponel V, Parchoux F *et al.* 2001. Late-glacial and Holocene high-altitude environmental changes in Vallée des Merveilles (Alpes–Maritimes, France): insect evidence. *Journal of Quaternary Science* **16**: 795–812. https://doi.org/10.1002/jqs.634

Protin M, Schimmelpfennig I, Mugnier JL *et al.* 2019. Climatic reconstruction for the Younger Dryas/Early Holocene transition and the Little Ice Age based on paleo-extents of Argentière glacier

(French Alps). *Quaternary Science Reviews* **221**. https://doi.org/10.1016/j.quascirev.2019.105863 [PubMed: 105863]

Rea BR, Pellitero R, Spagnolo M *et al.* 2020. Atmospheric circulation over Europe during the Younger Dryas. *Science Advances* **6**: eaba4844. https://doi.org/10.1126/sciadv.aba4844 [PubMed: 33310841]

Regattieri E, Zanchetta G, Isola I *et al.* 2019. Holocene Critical Zone dynamics in an Alpine catchment inferred from a speleothem multiproxy record: disentangling climate and human influences. *Scientific Reports* **9**: 17829. https://doi.org/10.1038/s41598-019-53583-7 [PubMed: 31780672]

Reinig F, Wacker L, Jöris O *et al.* 2021. Precise date for the Laacher See eruption synchronizes the Younger Dryas. *Nature* **595**: 66–69. https://doi.org/10.1038/s41586-021-03608-x [PubMed: 34194020]

Ribolini A, Chelli A, Guglielmin M *et al.* 2007. Relationships between glacier and rock glacier in the Maritime Alps, Schiantala Valley, Italy. *Quaternary Research* **68**: 353–363. https://doi.org/10.1016/j.yqres.2007.08.004

Roberts CN, Zanchetta G, Jones MD. 2010. Oxygen isotopes as tracers of Mediterranean climate variability: an introduction. *Global and Planetary Change* **71**: 135–140. https://doi.org/10.1016/j.gloplacha.2010.01.024

Roberts N, Eastwood WJ, Kuzucuoğlu C *et al.* 2011. Climatic, vegetation and cultural change in the eastern Mediterranean during the mid-. *Holocene environmental transition. Holocene* **21**: 147–162. https://doi.org/10.1177/0959683610386819

Roberts N, Jones MD, Benkaddour A *et al.* 2008. Stable isotope records of Late Quaternary climate and hydrology from Mediterranean lakes: the ISOMED synthesis. *Quaternary Science Reviews* **27**: 2426–2441. https://doi.org/10.1016/j.quascirev.2008.09.005

SAGE. 2014. PAGD du SAGE Verdon approuvé par arrêté inter préfectoral du 13 octobre 2014. Available at: https://www.gesteau.fr/document/plan-damenagement-et-de-gestion-durable-du-sage-verdon.

Samartin S, Heiri O, Vescovi E *et al.* 2012. Lateglacial and Early Holocene summer temperatures in the southern Swiss Alps reconstructed using fossil chironomids. *Journal of Quaternary Science* **27**: 279–289. https://doi.org/10.1002/jqs.1542

Schürch M, Kozel R, Schotterer U *et al.* 2003. Observation of isotopes in the water cycle?the Swiss National Network (NISOT). *Environmental Geology* **45**: 1–11. https://doi.org/10.1007/s00254-003-0843-9

Schwander J, Eicher U, Ammann B. 2000. Oxygen isotopes of lake marl at Gerzensee and Leysin (Switzerland), covering the Younger Dryas and two minor oscillations, and their correlation to the GRIP ice core. *Palaeogeography, Palaeoclimatology, Palaeoecology* **159**: 203–214. https://doi.org/10.1016/S0031-0182(00)00085-7

Sivan O, Miramont C, Edouard J-L. 2006. Rythmes de la sédimentation et interprétations paléoclimatiques lors du Postglaciaire (Alpes du Sud) 14c et dendro-géomorphologie, deux chronomètres complémentaires. *L'Erosion entre Société, Climat et Paléoenvironnement*. Paper presented at the Round Table in honor of René NEBOIT-GUILHOT. Presses Universitaires Blaise-Pascal: Clermont-Ferrand; 423–428.

Spagnolo M, Ribolini A. 2019. Glacier extent and climate in the Maritime Alps during the Younger Dryas. *Palaeogeography, Palaeoclimatology, Palaeoecology* **536**. https://doi.org/10.1016/j.palaeo.2019.109400 [PubMed: 109400]

Stuiver M. 1970. Oxygen and carbon isotope ratios of fresh-water carbonates as climatic indicators. *Journal of Geophysical Research* **75**: 5247–5257. https://doi.org/10.1029/JC075i027p05247

Tang K, Feng X. 2001. The effect of soil hydrology on the oxygen and hydrogen isotopic compositions of plants' source water. *Earth and Planetary Science Letters* **185**: 355–367. https://doi.org/10.1016/S0012-821X(00)00385-X

von Grafenstein U, Belmecheri S, Eicher U *et al.* 2013. The oxygen and carbon isotopic signatures of biogenic carbonates in Gerzensee, Switzerland, during the rapid warming around 14,685 years BP and the following interstadial. *Palaeogeography, Palaeoclimatology, Palaeoecology* **391**: 25–32. https://doi.org/10.1016/j.palaeo.2013.08.018

von Grafenstein U, Erlenkeuser H, Müller J *et al.* 1996. A 200 year mid-European air temperature record preserved in lake sediments: an extension of the δ18Op-air temperature relation into the past. *Geochimica et Cosmochimica Acta* **60**: 4025–4036. https://doi.org/10.1016/S0016-7037(96)00230-X

von von Grafenstein UU, Erlenkeuser H, Brauer A *et al.* 1999. A mid-European decadal isotope-climate record from 15,500 to 5000 years B.P. *Science* **284**: 1654–1657. https://doi.org/10.1126/science.284.5420.1654 [PubMed: 10356392]

Walker M, Head MJ, Berkelhammer M *et al.* 2018. Formal ratification of the subdivision of the Holocene Series/Epoch (Quaternary System/Period): two new Global Boundary Stratotype Sections and Points (GSSPs) and three new stages/subseries. *Episodes* **41**: 213–223. https://doi.org/10.18814/epiiugs/2018/018016

Wilhelm B, Arnaud F, Sabatier P *et al.* 2012. 1400 years of extreme precipitation patterns over the Mediterranean French Alps and possible forcing mechanisms. *Quaternary Research* **78**: 1–12. https://doi.org/10.1016/j.yqres.2012.03.003

Wirth SB, Glur L, Gilli A *et al.* 2013. Holocene flood frequency across the Central Alps – solar forcing and evidence for variations in North Atlantic atmospheric circulation. *Quaternary Science Reviews* **80**: 112–128. https://doi.org/10.1016/j.quascirev.2013.09.002

Wirth SB, Sessions AL. 2016. Plant-wax D/H ratios in the southern European Alps record multiple aspects of climate variability. *Quaternary Science Reviews* **148**: 176–191. https://doi.org/10.1016/j.quascirev.2016.07.020

Zanchetta G, Drysdale RN, Hellstrom JC *et al.* 2007. Enhanced rainfall in the western Mediterranean during deposition of sapropel S1: stalagmite evidence from Corchia cave (Central Italy). *Quaternary Science Reviews* **26**: 279–286. https://doi.org/10.1016/j.quascirev.2006.12.003